Electronic Supplementary Material (ESI) for Journal of Materials Chemistry A.

Supporting Information

Structural Rule of N-Coordinated Single Atomic Catalysts for Electrochemical CO_2 Reduction

Zhenxin Lou[a], Wenjing Li[a], Haiyang Yuan[*ab], Yu Hou[a], Huagui Yang[a], Haifeng Wang[*b]

[a]Key Laboratory for Ultrafine Materials of Ministry of Education, Shanghai Engineering Research Center of Hierarchical Nanomaterials, School of Materials Science and Engineering, East China University of Science and Technology, Shanghai 200237, China.

[b]Key Laboratory for Advanced Materials, Research Institute of Industrial Catalysis and Center for Computational Chemistry, School of Chemistry and Molecular Engineering, East China University of Science and Technology, Shanghai, 200237, China.

*Emails: hfwang@ecust.edu.cn; hyyuan@ecust.edu.cn

Note S1. Computational Methodology

The electrochemical conversion of CO_2 into CO (CO_2RR) involves the transfer of two proton-coupled electron pairs and three key intermediates (*CO_2, *COOH and *CO), whose four elementary steps can be written as:

$$* + CO_{2(g)} \rightarrow *CO_2 \quad (1)$$

$$*CO_2 + H^+/e^- \rightarrow *COOH \quad (2)$$

$$*COOH + H^+/e^- \rightarrow *CO + H_2O \quad (3)$$

$$*CO \rightarrow * + CO_{(g)} \quad (4)$$

Here, we calculated the adsorption energies of the key intermediates in the CO_2RR process with the formula: $E_{ads}(X) = E_{X/surf} - E_{surf} - E_X$, where $E_{X/surf}$, E_{surf} and E_X represent the energies of the surface with adsorbates, the clean substrate, and adsorbates, respectively. For *COOH, E_{ads}(*COOH) was calculated by reference to the energies of CO_2 and $1/2H_2$ according to the computational hydrogen electrode (CHE) model. The more negative $E_{ads}(X)$ indicates the stronger binding strength between adsorbates and the surface.

The Gibbs free energy changes (ΔG) of elementary steps in CO_2RR were calculated using the CHE model. In this approach, the chemical potentials of a proton-electron pair (H^+/e^-) and half H_2 molecule are equilibrated at 0 V (vs. the reversible hydrogen electrode, RHE) at all pH values.[1, 2] The effect of the potential on the state with an electron involved was considered by shifting the energy of $-eU$. Therefore, after obtaining the adsorption energy of the key intermediates, the corresponding Gibbs free energy change (ΔG_i) of each elementary step in CO_2RR at the potential U can be calculated as follows:

$$\Delta G_1 = E(*CO_2) - E(*) - E(CO_{2(g)}) + (\Delta E_{ZPE} - T\Delta S) \quad (5)$$
$$= E_{ads}(*CO_2) + (\Delta E_{ZPE} - T\Delta S)$$

$$\Delta G_2 = E(*COOH) - E(*CO_2) - E(H_2)/2 + (\Delta E_{ZPE} - T\Delta S) + eU \quad (6)$$
$$= E_{ads}(*COOH) - E_{ads}(*CO_2) + (\Delta E_{ZPE} - T\Delta S) + eU$$

$$\Delta G_3 = E(*CO) + E(H_2O) - E(*COOH) - E(H_2)/2 + (\Delta E_{ZPE} - T\Delta S) + eU \quad (7)$$
$$= E_{ads}(*CO) - E_{ads}(*COOH) + (\Delta E_{ZPE} - T\Delta S) + \Delta G_0 + eU$$

$$\Delta G_4 = E(*) + E(CO_{(g)}) - E(*CO) + (\Delta E_{ZPE} - T\Delta S) \quad (8)$$
$$= - E_{ads}(*CO) + (\Delta E_{ZPE} - T\Delta S)$$

where E_{ads}(*CO_2), E_{ads}(*COOH) and E_{ads}(*CO) are the adsorption energies of *CO_2, *COOH and *CO, and ΔG_0 is the Gibbs free energy of CO_2RR to CO from the experiment ($CO_2 + H_2 \rightarrow CO + H_2O$, ΔG_0 = 0.67 eV). ΔE_{ZPE} and $T\Delta S$ are the differences of the zero-point energy and entropic contributions (see the detailed data in Table S2), which result from the experimental data and vibrational frequency calculations at 298 K. Theoretically, the reaction maximum Gibbs free energy (ΔG_{CO2RR}) of the elementary steps in CO_2RR is often used to evaluate the intrinsic activities of catalysts, which can be written as $\Delta G_{CO2RR} = \max\{\Delta G_1, \Delta G_2, \Delta G_3, \Delta G_4\}$

With respect to the effect of the solution, we employed the implicit CANDLE solvation model by JDFTx software upon all structures, using the Garrity–Bennett–Rabe–Vanderbilt (GBRV) ultrasoft pseudopotentials (USPP).[3, 4] We corrected the solvation energy resulting from JDFTx into Gibbs free energy change (ΔG_i) of each elementary step in CO_2RR to estimate the effect of solvent. Taking Co, W and Ru GN_x SACs (x = 2, 3, 4) as examples, Table S3 lists ΔG_i with or without solvent involved and the corresponding difference (Δ, i.e., the solvation correction). It can be observed that all Δ are around or even smaller than 0.1 eV, which contributes a little effect to the qualitative identification

of the activity trend of TM-GN_x (x = 2, 3, 4). Therefore, the solvent-induced effect toward the related adsorbates is small, and contributes little effect to the tendency judgment.

Table S1. The specific applied *U*-*J* value (U_{eff}) of 3*d* metals for DFT calculations.[6]

3*d*	Cr	Mn	Fe	Co	Ni
U_{eff}	2.79	3.06	3.29	3.42	3.40

Table S2. Zero-point energies (E_{ZPE}) and entropies (TS) of gas molecules and key intermediates at 298 K.

	Species	E_{ZPE}	TS
	H_2O	0.57	0.67
	H_2	0.27	0.41
	CO_2	0.13	0.66
	CO	0.07	0.61
	*	0.32	0.10
	*CO_2	0.63	0.40
TM- GN_2	*COOH	0.93	0.29
	*CO	0.55	0.23
	*H	0.49	0.00
	*	0.48	0.13
	*CO_2	0.77	0.27
TM- GN_3	*COOH	1.08	0.33
	*CO	0.66	0.35
	*H	0.66	0.00
	*	0.60	0.16
	*CO_2	0.88	0.32
TM- GN_4	*COOH	1.22	0.32
	*CO	0.81	0.33
	*H	0.76	0.00

Table S3. Gibbs free energy change (Δ*G*) of each elementary step of CO_2RR into CO on TM-GN_x with or without solvent involved, and the corresponding difference (**Δ**). The unit is eV.

			* + CO_2(g) → *CO_2	*CO_2 + H^+/e^- → *COOH	*COOH + H^+/e^- → *CO + H_2O	*CO → * + CO(g)
Co	GN_2	no-solvent	0.38	0.45	-0.66	0.59
		solvent	0.36	0.35	-0.79	0.62
		Δ	**-0.02**	**-0.11**	**-0.13**	**0.03**
	GN_3	no-solvent	0.32	-0.11	-1.06	1.62
		solvent	0.33	-0.19	-1.15	1.54
		Δ	**0.01**	**-0.07**	**-0.09**	**-0.08**
	GN_4	no-solvent	0.38	0.72	-0.27	-0.06
		solvent	0.32	0.67	-0.34	-0.12
		Δ	**-0.06**	**-0.04**	**-0.07**	**-0.06**
Ru	GN_2	no-solvent	0.27	-0.28	-0.88	1.65
		solvent	0.31	-0.39	-1.01	1.63
		Δ	**0.04**	**-0.12**	**-0.13**	**-0.02**
	GN_3	no-solvent	-0.30	-0.09	-0.78	1.94
		solvent	-0.27	-0.22	-0.87	1.89
		Δ	**0.04**	**-0.12**	**-0.10**	**-0.05**
	GN_4	no-solvent	0.03	0.04	-1.33	2.03
		solvent	-0.08	-0.05	-1.43	2.10
		Δ	**-0.11**	**-0.09**	**-0.10**	**0.07**
W	GN_2	no-solvent	0.18	-0.14	-1.03	1.75
		solvent	0.25	-0.28	-1.12	1.68
		Δ	**0.08**	**-0.14**	**-0.10**	**-0.07**
	GN_3	no-solvent	-0.77	-0.26	-0.30	2.09
		solvent	-0.70	-0.39	-0.42	2.04
		Δ	**0.06**	**-0.13**	**-0.12**	**-0.05**
	GN_4	no-solvent	-0.26	-0.54	-0.41	1.97
		solvent	-0.34	-0.51	-0.52	1.90
		Δ	**-0.08**	**0.03**	**-0.11**	**-0.07**

Note S2. Stability of TM-GN_x

The formation energy (E_f) and dissolution potential (U_{diss}) of TM-GN_x (x = 2, 3, 4) were examined, which can be used to assess the thermodynamic and electrochemical stabilities, respectively. The relevant formulas are as follows:[5]

$$E_f = E_b - E_c = (E_{TM\text{-}GN} - E_{GN} - E_{TM}) - E_c \quad (9)$$

$$U_{diss} = U_{diss}^{o} - E_f/(ne) \quad (10)$$

where E_b and E_c are the binding energy of metal center (TM) with substrate and the cohesive energy of metal; $E_{TM\text{-}GN}$, $E_{M\text{-}GN}$, E_{GN} and E_M are the energies of the substrate GN with single metal atom anchored, pure substrate GN and single metal atom, respectively; n is the number of electrons involved in the dissolution process; U_{diss}^{o} is the standard dissolution potential of metal from experiments.[5]

According to the definition, the more negative E_f and more positive U_{diss} means the more superior thermodynamic and electrochemical stabilities, respectively[5]. From Figure S1, we can see that TM-GN_4 generally has the best thermodynamic and electrochemical stability compared to M-GN_2 and M-GN_3 (TM-GN_4 > TM-GN_2 > TM-GN_3), which have the most negative E_f and positive U_{diss}. This result can be rationalized from the structural properties of GN_x (x = 2 ~ 4). Structurally, both GN_2 (or GN_4) are the coplanar topological structure; TM on GN_2 is in the linear configuration bonded by two N atoms, while on GN_4, TM is saturated by four N atoms. Thus, the interaction of metal center with GN_2 is relatively weaker than that with GN_4, which is well demonstrated by the stronger E_b and shorter TM-N bonds, as Table S4 illustrates. For GN_3, due to the relatively narrow space, the metal center is pushed out of the graphene layer, forming a tapered configuration with a relatively weak interaction, which would be easy to transfer and agglomerate with each other on nitrogen-doped carbons.

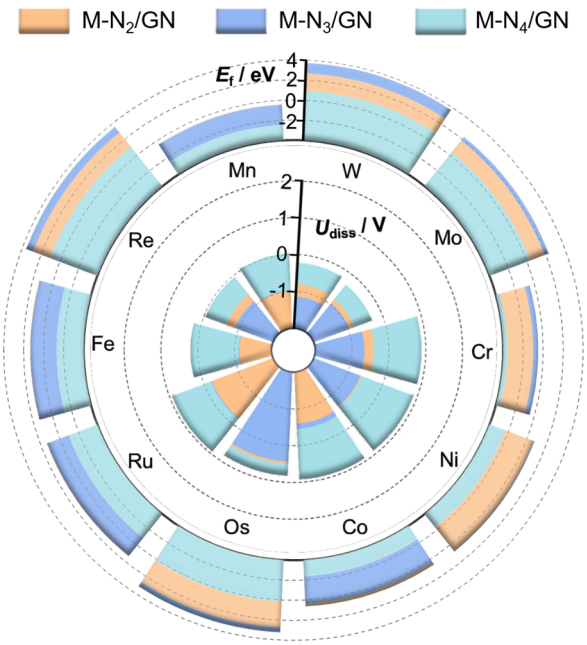

Figure S1. Calculated formation energies (E_f) and dissolution potential (U_{diss}) of different TM-GN_x, where orange, blue and green represent TM-GN_x (x = 2, 3, 4), respectively.

Table S4. Calculated binding energies (E_b) and bond length of TM with GN_2 and GN_4. E_b was calculated according to the following formula: $E_b = E_{TM/sub} - E_{sub} - E_{TM}$, where $E_{TM/sub}$, E_{sub} and E_{TM} are the energies of the substrate with metal atom anchored, substrates (GN_2 and GN_4) and single metal atom., respectively.

	E_b (eV)		TM-N Bond (Å)	
	GN_2	GN_4	GN_2	GN_4
Cr	-5.09	-7.68	1.975	1.961
Mn	-3.33	-5.38	1.950	1.909
Fe	-2.92	-5.58	2.148	1.908
Co	-3.76	-6.78	1.892	1.889
Ni	-3.73	-6.74	1.904	1.882
Mo	-4.96	-6.47	2.041	2.038
Ru	-5.36	-7.67	1.982	1.972
W	-6.21	-7.97	2.015	2.001
Re	-5.16	-6.98	2.005	1.969
Os	-5.46	-8.02	1.977	1.941

Table S5. Calculated cohesive energies (E_c) and the corresponding experimental ($E_c^{exp.}$) values.

Metal	E_c	$E_c^{exp.}$
Ti	-5.54	-4.85
Zr	-6.38	-6.25
Hf	-6.54	-6.44
V	-6.33	-5.31
Nb	-6.92	-7.57
Ta	-8.17	-8.10
Cr	-4.16	-4.10
Mo	-6.26	-6.82
W	-8.41	-8.90
Mn	-3.99	-2.92
Re	-7.82	-8.03
Fe	-4.76	-4.28
Ru	-7.19	-6.74
Os	-8.31	-8.17
Co	-5.21	-4.39
Rh	-5.95	-5.75
Ir	-7.28	-6.94
Ni	-5.17	-4.44
Pd	-3.70	-3.89
Pt	-5.43	-5.84
Cu	-3.86	-3.49
Au	-3.62	-3.81
Ag	-2.95	-2.95

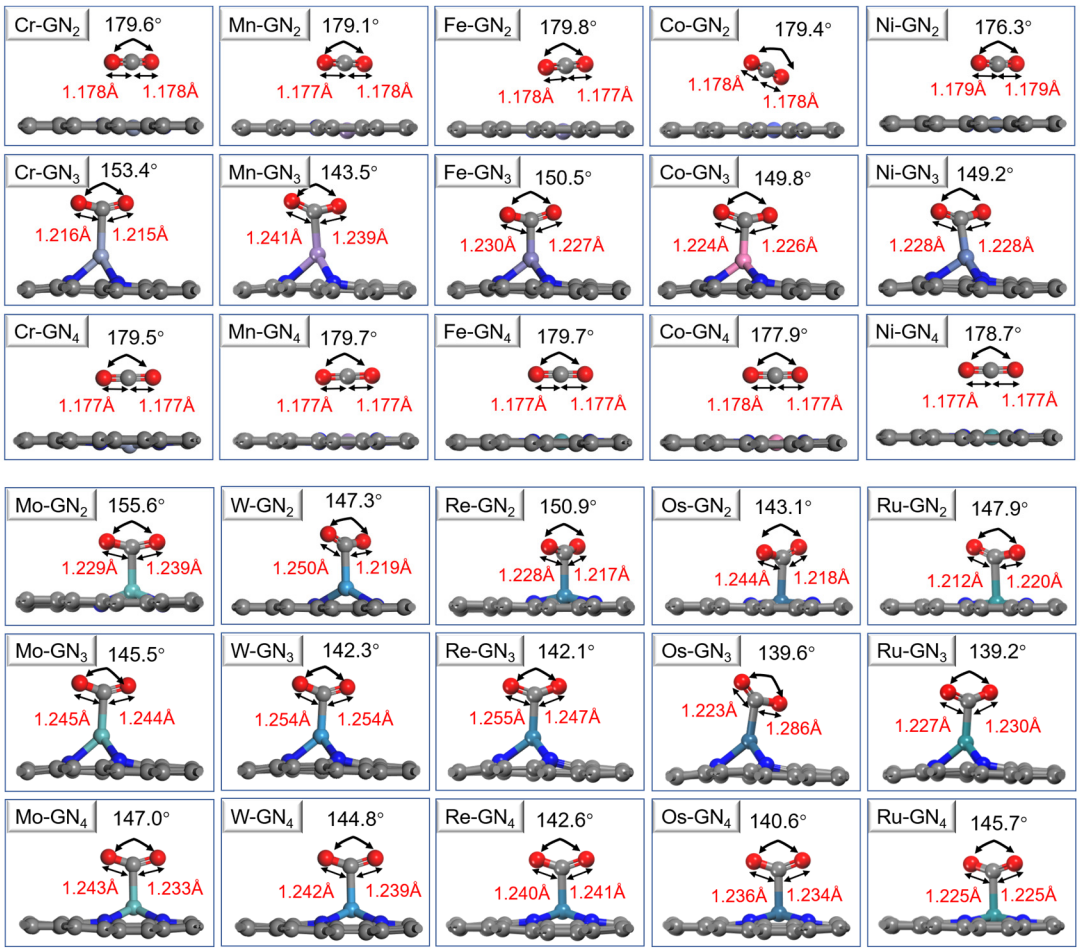

Figure S2. Adsorption configurations of CO_2 on the transition metal SACs anchored on nitrogen-doped graphene (TM-GN_x, x = 2, 3 and 4).

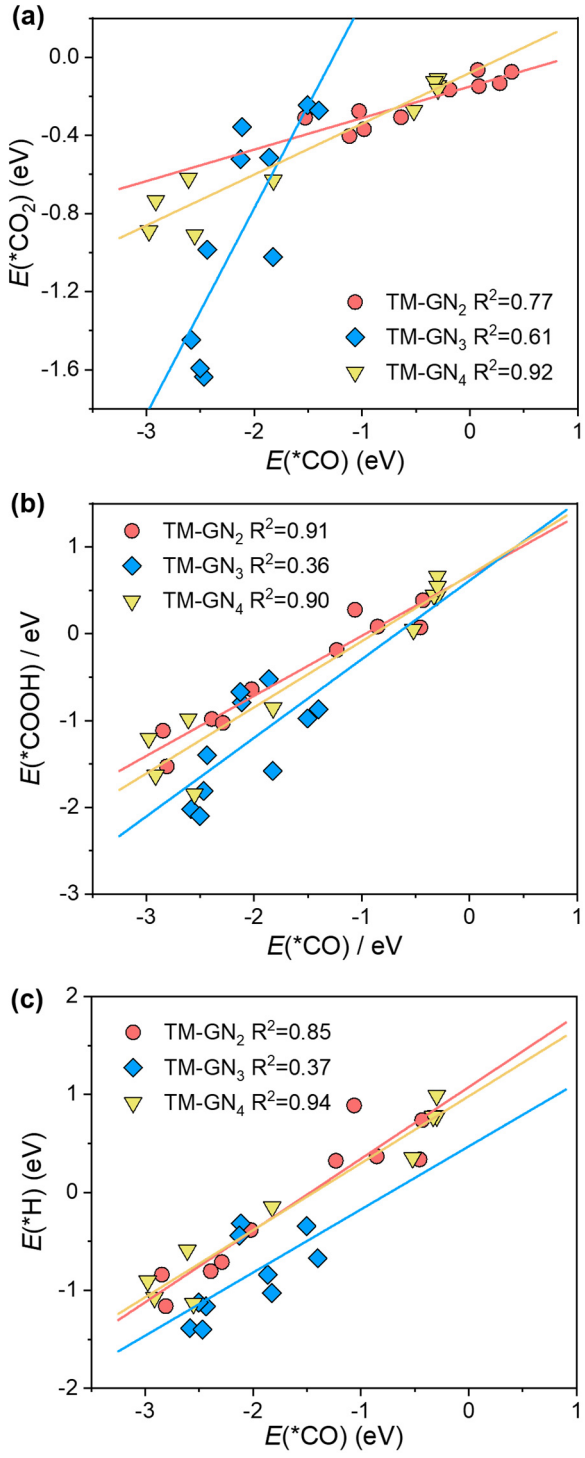

Figure S3. Calculated scaling relationship about the adsorption energy of key intermediates in terms of the descriptor *E*(*CO).

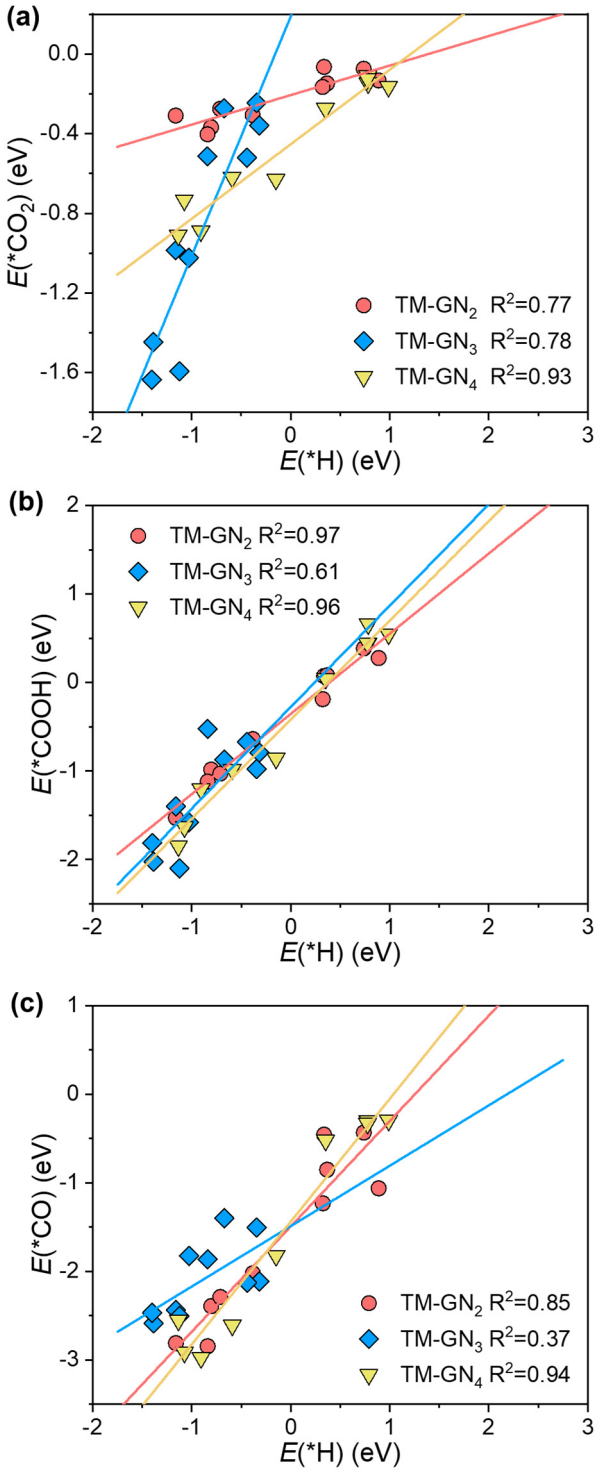

Figure S4. Calculated scaling relationship about the adsorption energy of key intermediates in terms of the descriptor *E*(*H).

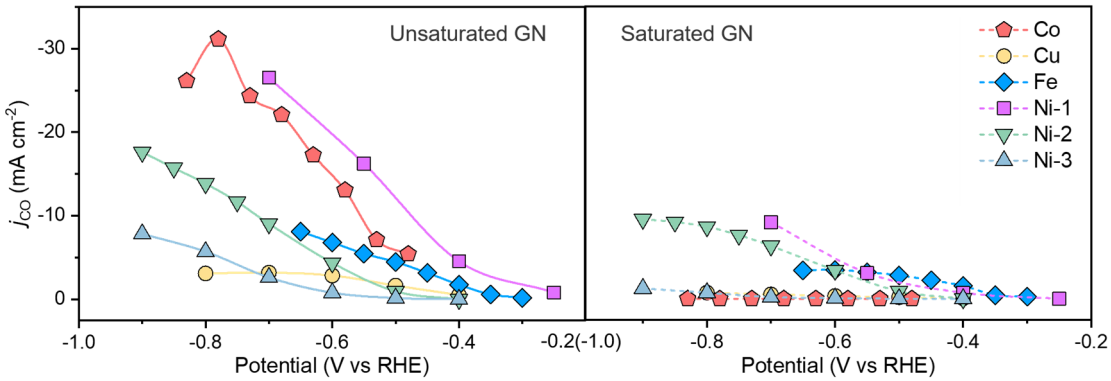

Figure S5. Partial current densities of CO on Fe (ref 65), Co (ref 66), Ni (ref 32, 36 and 58) and Cu (ref 34) SACs reported in experiments.

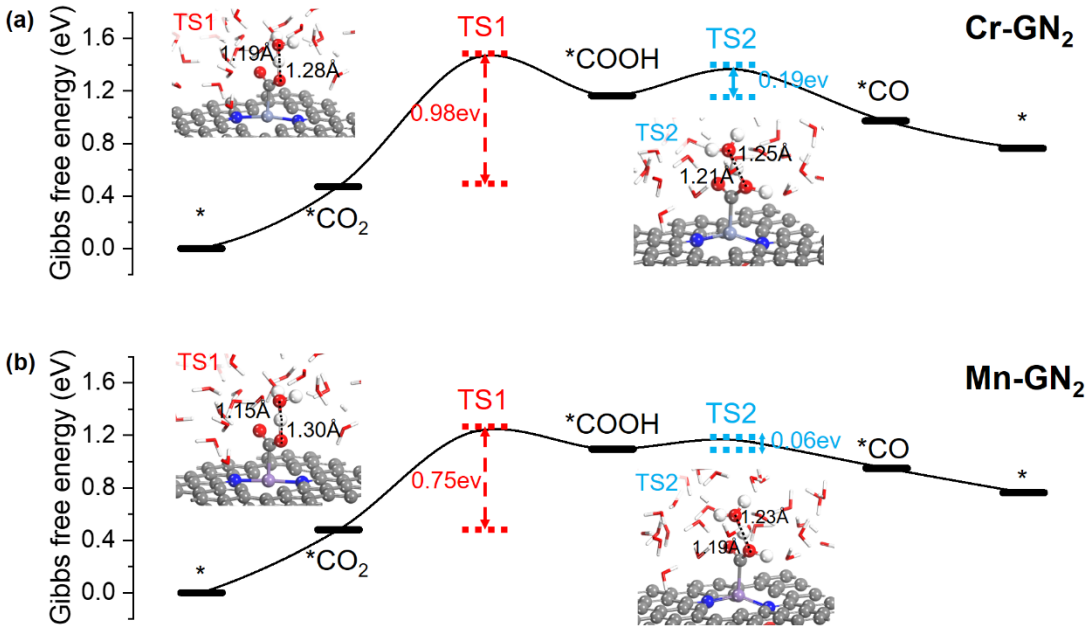

Figure S6. Energy profiles with the activation barriers considered of CO_2RR to CO on the unsaturated N-coordinated Cr-GN_2 (a), Mn-GN_2 (b), and the optimized structures of the transition states (TS) of the $*CO_2$ hydrogenation into *COOH ($*CO_2 + H^+/e^- \rightarrow$ *COOH) and *COOH hydrogenation into *CO ($*CO_2 + H^+/e^- \rightarrow *CO + H_2O$). All of the TS were searched by a constrained optimization scheme.[7, 8]

Reference

1. J. K. Nørskov, J. Rossmeisl, A. Logadottir, L. Lindqvist, J. R. Kitchin, T. Bligaard and H. Jónsson, *J. Phys. Chem. B*, 2004, **108**, 17886.
2. A. J. Garza, A. T. Bell and M. Head-Gordon, *ACS Catal.*, 2018, **8**, 1490.
3. R. Sundararaman and W. A. Goddard, 3rd, *J Chem. Phys.*, 2015, **142**, 064107.
4. R. Sundararaman, K. Letchworth-Weaver, K. A. Schwarz, D. Gunceler, Y. Ozhabes and T. A. Arias, *Softwarex*, 2017, **6**, 278-284.
5. X. Guo, J. Gu, S. Lin, S. Zhang, Z. Chen and S. Huang, *J. Am. Chem. Soc.*, 2020, **142**, 5709-5721.
6. C. Y. Lin, L. Zhang, Z. Zhao and Z. Xia, *Adv. Mater.*, 2017, **29**, 1606635.
7. H. Yuan, N. Sun, J. Chen, J. Jin, H. Wang and P. Hu, *ACS Catalysis*, 2018, **8**, 9269-9279.
8. D. Wang, T. Sheng, J. Chen, H.-F. Wang and P. Hu, *Nature Catalysis*, 2018, **1**, 291-299.